

# AN INVESTIGATION OF UNIFORM EXPANSIONS OF LARGE ORDER BESSEL FUNCTIONS IN GRAVITATIONAL WAVE SIGNALS FROM PULSARS

F.A. Chishtie<sup>†</sup>, K.M. Rao<sup>†</sup>, I.S. Kotsireas<sup>\*</sup>, S.R. Valluri<sup>‡</sup>

Departments of <sup>†</sup>Applied Mathematics, <sup>‡</sup>Physics & Astronomy, University of Western Ontario, London, Canada

<sup>\*</sup>Department of Physics and Computer Science, Wilfrid Laurier University, Waterloo, Canada  
E-mail: farrukh4ad@yahoo.com, krao@uwo.ca, ikotsire@wlu.ca, valluri@uwo.ca

## Abstract

In this work, we extend the analytic treatment of Bessel functions of large order and/or argument. We examine uniform asymptotic Bessel function expansions and show their accuracy and range of validity. Such situations arise in a variety of applications, in particular the Fourier transform of the gravitational wave signal from a pulsar. The uniform expansion we consider here is found to be valid in the entire range of the argument.

## 1 Introduction

The detection of gravitational waves (GW) from astrophysical sources is one of the most important problems in experimental gravitation today. Large laser interferometric gravitational wave detectors like LIGO, VIRGO, LISA, TAMA 300, GEO 600 and AIGO may in the near future open a new window for the study of a great variety of nonlinear curvature phenomena.

In recent works [1, 2, 3] we have analyzed the Fourier transform (FT) of the Doppler shifted GW signal from a pulsar with the use of the plane wave expansion in spherical harmonics (PWESH), which has a variety of applications in many areas [4, 5, 6]. The consequent analysis of the Fourier transform of the GW signal from a pulsar has a very interesting and convenient development in terms of the resulting spherical Bessel, generalized hypergeometric, gamma and Legendre functions. Both rotational and orbital motions of the Earth and spindown of the pulsar can be considered in this analysis which happens to have a nice analytic representation for the GW signal in terms of the above special functions. The signal can then be studied as a function of a variety of different parameters associated with both the GW pulsar signal as well as the orbital and rotational parameters. The numerical analysis of this analytical expression for the signal offers a challenge for fast and high performance parallel computation. Recent studies of the Cosmic Microwave Background Explorer have raised the interesting question of the study of very large multipole moments with angular momentum  $l$  and its projection  $m$  going up to very large values of  $l \sim 1000$ . Such problems warrant an intensive analytic study supplemented by numerical and parallel computation.

Since our FT depends on the Bessel function, a computational issue arises due to large values of the index or order  $n$  of the function. In the GW form of the pulsar, the Doppler shifted orbiting motion gives rise to Bessel functions  $J_n\left(\frac{2\pi f_0 A \sin \theta}{c}\right)$ , where  $\frac{2\pi f_0 A \sin \theta}{c}$  is large for non-negligible angle  $\theta$ . Even for  $\sin \theta \sim \frac{1}{1000}$ , the argument is large necessitating the consideration of large values of  $n$ . The motivation of this work is to extend the analysis in Watson [7] for large index, argument and overlapping situations. Meissel [8] has made derivations for large order Bessel functions both when the argument is smaller than the order and vice versa. These were studied in the GW context in an earlier work by us [9]. We extend this study by considering another type of expansion, also referred to as the “uniform” Bessel expansion, which, being an expansion in the Airy functions, allows for single series form, hence the name [10]. As an application, we will address the phenomenological situation of GW signal analysis of large order  $n$  (which does arise with combinations of  $l$  and  $m$ ).

The expansion in terms of the Bessel functions has recently found a valuable application [11] in the identification of global parameter space correlations of a coherent matched filtering search for continuous GW from isolated neutron stars. The authors have done an interesting pioneering analysis of the global correlations and indicate that the locations of local maxima of the detection statistics involve Bessel functions and are dominated by the Doppler shift due to the Earth's orbital motion. We have made a preliminary extension of their analysis that makes use of the summation of infinite series involving Bessel functions and other relevant functions of the parameters and physical variables. Their various levels of approximation can be further improved for a comparison with exact numerical results.

Captures of stellar-mass compact objects (CO) by massive black holes are important capture sources for the Laser Interferometer Space Antenna (LISA), the space based GW detector due to be launched in about a decade [12]. Higher Harmonics of the orbital frequency of the COs arise in the post Newtonian (PN) capture GW model forms and contribute considerably to the total signal to noise (S/N) ratio of the waveform. The GW form can be decomposed into gravitational multipole moments which are treated in the Fourier analysis of Keplerian eccentric orbits. The radiation depends strongly on the orbital eccentricity  $e$ , and Bessel functions  $J_n(ne)$  are a natural consequence of the analysis. Such calculations involving gravitational wave forms necessitate a very accurate evaluation of Bessel functions of large order and argument due to the importance of orbital eccentricity. Accurate and efficient evaluations of Bessel functions for constructing reliable gravitational wave templates from binary stars with arbitrary orbital eccentricity have been done by Pierro et al. [13] using generalized Carlini-Meissel expansions. The methods investigated in the current work can also be applied to such calculations relating to LISA capture sources.

The calculation of partial derivatives of the potential scattering phase shifts which often contain Bessel and Legendre functions of large order angular momentum  $l$ , with respect to angular momentum arise in a variety of scattering problems in atomic, molecular and nuclear physics. In particular, large values of  $l$  can arise in rainbow, glory and orbit scattering [14, 15], in black hole gravitational fields [16], and in catastrophe theory [17]. The analysis in our paper should help provide suitable approximations for large order and/or argument for the Bessel functions that arise in such problems.

In section 2 we give the relevant expressions from our work on GW signal analysis to demonstrate the occurrence of large order Bessel functions. Section 3 presents the uniform expansion and the expressions associated with it. We discuss the results in Section 4 and compare them with other expansions and the exact values of the Bessel functions.

## 2 Fourier Transform of the GW signal

The FT for the GW Doppler shifted pulsar signal [1] is given as follows:

$$\tilde{h}(f) = S_{nlm}(\theta, \phi) = \sum_{n=-\infty}^{\infty} \sum_{l=0}^{\infty} \sum_{m=-l}^l \psi_0 \psi_1 \psi_2 \psi_3 \psi_4 \quad (1)$$

where

$$\psi_0(n, l, m, \theta, \phi) = 4\pi i^l Y_{lm}(\theta, \phi) N_{lm} P_l^m(\cos \alpha) \quad (2)$$

$$\psi_1(n, \theta, \phi) = T_{rE} \sqrt{\frac{\pi}{2}} e^{-i \frac{2\pi f_0 A}{c} \sin \theta \cos \phi} i^n e^{-in\phi} J_n \left( \frac{2\pi f_0 A \sin \theta}{c} \right) \quad (3)$$

$$\psi_2(l, n, m) = \left\{ \frac{1 - e^{i\pi(l-B_{orb})R}}{1 - e^{i\pi(l-B_{orb})}} \right\} \frac{e^{-iB_{orb}\frac{\pi}{2}}}{2^{2l}} \quad (4)$$

$$\psi_3(l, n, m) = k^{l+\frac{1}{2}} \frac{\Gamma(l+1)}{\Gamma\left(l+\frac{3}{2}\right) \Gamma\left(\frac{l+B_{orb}+2}{2}\right) \Gamma\left(\frac{l-B_{orb}+2}{2}\right)} \quad (5)$$

$$\psi_4(l, n, m) = {}_1F_3\left(l+1; l+\frac{3}{2}; \frac{l+B_{orb}+2}{2}, \frac{l-B_{orb}+2}{2}; \frac{-k^2}{16}\right) \quad (6)$$

Here  $\alpha$  is the co-latitude detector angle and angles  $\theta$  and  $\phi$  specify the direction of the pulsar source. Also  $\omega_0 = 2\pi f_0$ ,  $\omega_{orb} = \frac{2\pi}{T_{orb}}$  ( $T_{orb} = 365$  days),  $\omega_{rot} = \frac{2\pi}{T_{rE}}$  ( $T_{rE} = 1$  day),  $B_{orb} = 2\left(\frac{\omega-\omega_0}{\omega_{rot}} + \frac{m}{2} + \frac{n\omega_{orb}}{\omega_{rot}}\right)$ ,  $k = \frac{4\pi f_0 R_E \sin(\alpha)}{c}$  ( $R_E$  is the radius of Earth,  $c$  is the velocity of light) and  $A = 1.5 \times 10^{11}$  meters is the Sun-Earth distance.

### 3 Uniform expansion of the Bessel function

An expansion that approximates the Bessel function  $J_\nu(\nu z)$  for large  $\nu$ , which in principle is valid for all real values of  $z$ , is given in [10] as

$$J_\nu(\nu z) \sim \left(\frac{4\zeta}{1-z^2}\right)^{1/4} \left[ \frac{Ai(\nu^{2/3}\zeta)}{\nu^{1/3}} \sum_{k=0}^{\infty} \frac{a_k(\zeta)}{\nu^{2k}} + \frac{Ai'(\nu^{2/3}\zeta)}{\nu^{5/3}} \sum_{k=0}^{\infty} \frac{b_k(\zeta)}{\nu^{2k}} \right] \quad (7)$$

where

$$a_k(\zeta) = \sum_{s=0}^{2k} \mu_s \zeta^{-3s/2} u_{2k-s} (1-z^2)^{-1/2} \quad (8)$$

$$b_k(\zeta) = -\zeta^{-1/2} \sum_{s=0}^{2k+1} \lambda_s \zeta^{-3s/2} u_{2k-s+1} (1-z^2)^{-1/2} \quad (9)$$

$$\lambda_s = \frac{(2s+1)(2s+3)\dots(6s-1)}{s!(144)^s} \quad (10)$$

$$\mu_s = \frac{6s+1}{1-6s} \lambda_s \quad (11)$$

$$\frac{2}{3}\zeta^{3/2} = \ln\left(\frac{1+\sqrt{1-z^2}}{z}\right) - \sqrt{1-z^2} \quad (12)$$

$$\frac{2}{3}(-\zeta)^{3/2} = \sqrt{z^2 - 1} - \arccos\left(\frac{1}{z}\right) \quad (13)$$

$Ai(x)$  represents the Airy function. Equations 12 and 13 are used to define  $\zeta$ , the choice depending on the region of interest. Equation 12 is used when the argument of the Bessel function is less than the order, while equation 13 is used when the argument is larger than the order. Also, the  $u_i$  are defined recursively by

$$\begin{aligned} u_0(t) &= 1 \\ u_{k+1}(t) &= \frac{1}{2}t^2(1-t^2)u'_k(t) + \frac{1}{8}\int_0^t(1-5t^2)u_k(t)dt \quad (k = 0, 1, 2, \dots) \end{aligned}$$

Using the symbolic package MAPLE, we have computed these functions up to  $u_{11}$ , and the results are given below. They may, however, be calculated in principle up to any order, and MAPLE can perform this task fairly rapidly.

$$\begin{aligned} u_1 &= -\frac{5}{24}t^3 + \frac{1}{8}t \\ u_2 &= \frac{385}{1152}t^6 - \frac{77}{192}t^4 + \frac{9}{128}t^2 \\ u_3 &= -\frac{85085}{82944}t^9 + \frac{17017}{9216}t^7 - \frac{4563}{5120}t^5 + \frac{75}{1024}t^3 \\ u_4 &= \frac{37182145}{7962624}t^{12} - \frac{7436429}{663552}t^{10} + \frac{144001}{16384}t^8 - \frac{96833}{40960}t^6 + \frac{3675}{32768}t^4 \\ u_5 &= -\frac{5391411025}{191102976}t^{15} + \frac{5391411025}{63700992}t^{13} - \frac{108313205}{1179648}t^{11} + \frac{250881631}{5898240}t^9 - \frac{67608983}{9175040}t^7 + \frac{59535}{262144}t^5 \\ u_6 &= \frac{5849680962125}{27518828544}t^{18} - \frac{1169936192425}{1528823808}t^{16} + \frac{4445922195}{4194304}t^{14} - \frac{33010308331}{47185920}t^{12} + \frac{1441372804469}{6606028800}t^{10} - \\ &\quad \frac{388895895}{14680064}t^8 + \frac{2401245}{4194304}t^6 \\ u_7 &= -\frac{1267709431363375}{660451885056}t^{21} + \frac{1774793203908725}{220150628352}t^{19} - \frac{36927006432745}{2717908992}t^{17} + \frac{10559432785187}{905969664}t^{15} - \\ &\quad \frac{1602251736839}{301989888}t^{13} + \frac{1007390378503}{838860800}t^{11} - \frac{25388505925}{234881024}t^9 + \frac{57972915}{33554432}t^7 \\ u_8 &= \frac{2562040760785380875}{126806761930752}t^{24} - \frac{512408152157076175}{5283615080448}t^{22} + \frac{75358832548684685}{391378894848}t^{20} - \frac{39803268297948155}{195689447424}t^{18} + \\ &\quad \frac{3542717254441859}{28991029248}t^{16} - \frac{276439228010667}{6710886400}t^{14} + \frac{667955999804539}{93952409600}t^{12} - \frac{928090660435}{1879048192}t^{10} + \frac{13043905875}{2147483648}t^8 \\ u_9 &= -\frac{6653619855759634132375}{27390260577042432}t^{27} + \frac{1330723971151926826475}{1014454095446016}t^{25} - \frac{3128960418491082175}{1043677052928}t^{23} + \\ &\quad \frac{35348759075759093965}{9393093476352}t^{21} - \frac{17618708259302571707}{6262062317568}t^{19} + \frac{817138105244771959}{644245094400}t^{17} - \frac{3739063570455884033}{11274289152000}t^{15} + \\ &\quad \frac{1359491937582325}{30064771072}t^{13} - \frac{472414367256615}{188978561024}t^{11} + \frac{418854310875}{17179869184}t^9 \end{aligned}$$

$$\begin{aligned}
u_{10} &= \frac{4318199286388002551911375}{1314732507698036736} t^{30} - \frac{4318199286388002551911375}{219122084616339456} t^{28} + \frac{91891691150784941691275}{1803473947459584} t^{26} - \\
&\frac{16705838021516291703055}{225434243432448} t^{24} + \frac{19941766574064397067317}{300578991243264} t^{22} - \frac{5227733363217471800551}{139156940390400} t^{20} + \\
&\frac{1232816120293110459821}{92771293593600} t^{18} - \frac{35892416277828185849}{12884901888000} t^{16} + \frac{45660648644355162105}{148159191842816} t^{14} - \frac{20993386079260455}{1511828488192} t^{12} \\
&+ \frac{30241281245175}{274877906944} t^{10} \\
u_{11} &= -\frac{1556514560957130010757145625}{31553580184752881664} t^{33} + \frac{3424332034105686023665720375}{10517860061584293888} t^{31} - \frac{365967912305800454531456575}{389550372651270144} t^{29} \\
&+ \frac{201734750392525792544487385}{129850124217090048} t^{27} - \frac{11694306169843138084657687}{7213895789838336} t^{25} + \frac{164293183874328160710877}{148434069749760} t^{23} \\
&- \frac{23186185730591085896097833}{46756731971174400} t^{21} + \frac{527174389121818780771231}{3710851743744000} t^{19} - \frac{329641577686894230674187}{13469017440256000} t^{17} + \\
&\frac{241770821762631191867}{107752139522048} t^{15} - \frac{26416375998266454375}{314460325543936} t^{13} + \frac{1212400457192925}{2199023255552} t^{11}
\end{aligned}$$

In Table 1 we compare the values generated by this expansion with the exact Bessel function values, as well as the other expansions (Watson's expansion, epsilon expansion and Meissel's third expansion) from our previous work [9] for order  $\nu = 300$ . (Refer to the discussion section for the formulae for these expansions.) We also give a comparison for a larger order,  $\nu = 50000$ , in Table 2. We were not able to give exact values of the Bessel function for  $\nu = 50000$  due to the immense computational power required, but we give values for the other expansions for comparison.

Table 1: Comparison of expansions for  $J_\nu(x)$  with  $\nu = 300$ .

$x$	<b>290</b>	<b>295</b>	<b>298</b>	<b>302</b>	<b>305</b>	<b>310</b>
<b>Watson</b>	0.007669	0.027187	0.048992	0.084432	0.100255	0.057368
<b>Epsilon</b>	0.0076775	0.027215	0.049028	0.084335	0.10014	0.057419
<b>Uniform</b>	0.007677	0.027213	0.27573	-0.083138	0.10014	0.057419
<b>Exact</b>	0.007677	0.027215	0.049028	0.084335	0.10014	0.057419

Table 2: Comparison of expansions for  $J_\nu(x)$  with  $\nu = 50000$ .

$x$	<b>49800</b>	<b>49900</b>	<b>49999</b>	<b>50001</b>	<b>50100</b>	<b>50200</b>
<b>Watson</b>	$3.84377 \times 10^{-8}$	$1.02742 \times 10^{-4}$	0.011802	0.012444	-0.013648	0.001398
<b>Epsilon</b>	80.294	0.0016699	0.011839	0.012444	-0.012451	-6.3189
<b>Uniform</b>	$3.8445 \times 10^{-8}$	0.00010275	$8.7321 \times 10^{13}$	$3.8936 \times 10^{11}$	-0.013648	0.001398
<b>Exact</b>	N/A	N/A	N/A	N/A	N/A	N/A

The uniform expansion values were calculated using four terms in the series in equation 7. We note that there is a significant discrepancy between the uniform expansion values and the exact values close to the transition region. Temme [18] has noted that this is due to numerical singularities rather than to analytic singularities, and he has given expansions of the functions  $a_k(\zeta)$  and  $b_k(\zeta)$  appearing in equation 7. Using these improved formulae, we obtain the following uniform expansion values.

$x$	<b>290</b>	<b>295</b>	<b>298</b>	<b>302</b>	<b>305</b>	<b>310</b>
$\nu = 300$	0.00767703	0.027215	0.049028	0.084335	0.100143	0.057419
$x$	<b>49800</b>	<b>49900</b>	<b>49999</b>	<b>50001</b>	<b>50100</b>	<b>50200</b>
$\nu = 50000$	$3.844421 \times 10^{-8}$	0.00010275	0.011839	0.012444	-0.013648	0.0013977

A similar expansion for the first derivative of the Bessel function is also given in [10]. This expression is given below.

$$J'_\nu(\nu z) \sim -\frac{2}{z} \left( \frac{1-z^2}{4\zeta} \right)^{\frac{1}{4}} \left[ \frac{Ai(\nu^{2/3}\zeta)}{\nu^{4/3}} \sum_{k=0}^{\infty} \frac{c_k(\zeta)}{\nu^{2k}} + \frac{Ai'(\nu^{2/3}\zeta)}{\nu^{2/3}} \sum_{k=0}^{\infty} \frac{d_k(\zeta)}{\nu^{2k}} \right] \quad (14)$$

where

$$c_k(\zeta) = -\zeta^{\frac{1}{2}} \sum_{s=0}^{2k+1} \mu_s \zeta^{-3s/2} v_{2k-s+1} \left[ (1-z^2)^{-\frac{1}{2}} \right] \quad (15)$$

$$d_k(\zeta) = \sum_{s=0}^{2k} \lambda_s \zeta^{-3s/2} v_{2k-s} \left[ (1-z^2)^{-\frac{1}{2}} \right]. \quad (16)$$

The coefficients  $v_i$ , like  $u_i$ , are defined recursively, according to the following relation.

$$v_0(t) = 1$$

$$v_k(t) = u_k(t) + t(t^2 - 1) \left[ tu'_{k-1}(t) + \frac{1}{2}u_{k-1}(t) \right]$$

$$(k = 1, 2, \dots)$$

Using MAPLE, we have calculated these functions up to  $v_{11}$ , although generating higher order expressions is trivial, as is the case with  $u_i$ . We give these results below.

$$v_1 = \frac{7}{24}t^3 - \frac{3}{8}t$$

$$v_2 = -\frac{455}{1152}t^6 + \frac{33}{64}t^4 - \frac{15}{128}t^2$$

$$v_3 = \frac{95095}{82944}t^9 - \frac{6545}{3072}t^7 + \frac{5577}{5120}t^5 - \frac{105}{1024}t^3$$

$$v_4 = -\frac{40415375}{7962624}t^{12} + \frac{2739737}{221184}t^{10} - \frac{2448017}{245760}t^8 + \frac{114439}{40960}t^6 - \frac{4725}{32768}t^4$$

$$v_5 = \frac{5763232475}{191102976}t^{15} - \frac{215656441}{2359296}t^{13} + \frac{355886245}{3538944}t^{11} - \frac{280397117}{5898240}t^9 + \frac{15602073}{1835008}t^7 - \frac{72765}{262144}t^5$$

$$v_6 = -\frac{6183948445675}{27518828544}t^{18} + \frac{415138648925}{509607936}t^{16} - \frac{4775249765}{4194304}t^{14} + \frac{7176153985}{9437184}t^{12} - \frac{75861726551}{314572800}t^{10} +$$

$$\frac{440748681}{14680064}t^8 - \frac{2837835}{4194304}t^6$$

$$v_7 = \frac{1329548915820125}{660451885056}t^{21} - \frac{623575990562525}{73383542784}t^{19} + \frac{117495020467825}{8153726976}t^{17} - \frac{11287669528993}{905969664}t^{15} +$$

$$\frac{4806755210517}{838860800}t^{13} - \frac{23169978705569}{17616076800}t^{11} + \frac{28375388975}{234881024}t^9 - \frac{66891825}{33554432}t^7$$

$$v_8 = -\frac{2671063771882631125}{126806761930752}t^{24} + \frac{59582343274078625}{587068342272}t^{22} - \frac{237670164192005545}{1174136684544}t^{20} + \frac{42077740772116621}{195689447424}t^{18} -$$

$$\frac{1257093219318079}{9663676416}t^{16} + \frac{296916207863309}{6710886400}t^{14} - \frac{29041565208893}{3758096384}t^{12} + \frac{146540630595}{268435456}t^{10} - \frac{14783093325}{2147483648}t^8$$

$$v_9 = \frac{6904699850316601458125}{27390260577042432}t^{27} - \frac{461679745093525633675}{338151365148672}t^{25} + \frac{29412227933816172445}{9393093476352}t^{23} -$$

$$\frac{37073088786771732695}{9393093476352}t^{21} + \frac{6190356955971173843}{2087354105856}t^{19} - \frac{519996976064854883}{386547056640}t^{17} + \frac{3996930023590772587}{11274289152000}t^{15} -$$

$$\frac{1468251292588911}{30064771072}t^{13} + \frac{517406211757245}{188978561024}t^{11} - \frac{468131288625}{17179869184}t^9$$

$$v_{10} = -\frac{4464578923214714502823625}{1314732507698036736}t^{30} + \frac{1491741571661309972478475}{73040694872113152}t^{28} - \frac{286485860646564818213975}{5410421842378752}t^{26} +$$

$$\frac{17416724745836133903185}{225434243432448}t^{24} - \frac{2318810066751674077595}{33397665693696}t^{22} + \frac{16487466760916641832507}{417470821171200}t^{20} -$$

$$\frac{45614196450845087013377}{3246995275776000}t^{18} + \frac{12736018679229356269}{4294967296000}t^{16} - \frac{49042918914307396335}{148159191842816}t^{14} + \frac{22818897912239625}{1511828488192}t^{12}$$

$$- \frac{33424574007825}{274877906944}t^{10}$$

$$v_{11} = \frac{1604407316678887857241980875}{31553580184752881664}t^{33} - \frac{392956135061308232223935125}{1168651117953810432}t^{31} + \frac{1136426675054854043018733575}{1168651117953810432}t^{29} -$$

$$\frac{209347382482809784715977475}{129850124217090048}t^{27} + \frac{4057208263006803008962871}{2404631929946112}t^{25} - \frac{7721779642093423553411219}{6679533138739200}t^{23} +$$

$$\frac{24317219180863821793468459}{46756731971174400}t^{21} - \frac{185223434015774166216919}{1236950581248000}t^{19} + \frac{109880525895631410224729}{4233119766937600}t^{17} -$$

$$\frac{258444671539364377513}{107752139522048}t^{15} + \frac{28529686078127770725}{314460325543936}t^{13} - \frac{1327867167401775}{2199023255552}t^{11}$$

In Table 3 below, we compare the values of  $J'_\nu(x)$  obtained from the expansion with the exact values, for  $\nu = 300$ . A similar table is not given for  $\nu = 50000$  since we are not able to provide exact values for comparison, due to the large value of the index.

Table 3: Comparison of uniform expansion of  $J'_\nu(x)$  with exact values for  $\nu = 300$

$x$	<b>290</b>	<b>295</b>	<b>298</b>	<b>302</b>	<b>305</b>	<b>310</b>
<b>Uniform</b>	0.0021909	0.0059599	-0.010098	-0.019458	0.0014413	-0.018938
<b>Exact</b>	0.0021909	0.0059597	0.0084469	0.008023	0.0014411	-0.018938

## 4 Discussion

We find that the uniform expansions are accurate to a higher domain of validity than the expansions considered in our earlier work [9], thereby increasing their utility especially in the problematic  $z \sim 1$  or “transition” region. We compare the uniform expansion with the exact Bessel function values in the transition region in Figures 2 and 3 at the end of this section, which are plotted for order  $\nu = 300$ . It is seen that the uniform expansion agrees with the exact Bessel function curve for the entire range of the argument.

Previously, we presented two methods that are geared to work specifically in the transition region [9]. First, we present the results by Watson [7]. For the case of the argument being less than the order, he obtained, through the use of contour integration,

$$J_\nu(\nu \operatorname{sech}(\alpha)) = \frac{\tanh \alpha}{\pi\sqrt{3}} \exp \left[ \nu \left( \tanh \alpha + \frac{1}{3} \tanh^3 \alpha - \alpha \right) \right] K_{\frac{1}{3}} \left( \frac{1}{3} \nu \tanh^3 \alpha \right) + 3\theta_1 \nu^{-1} \exp[\nu(\tanh \alpha - \alpha)] \quad (17)$$

where  $|\theta_1| < 1$ . Similarly, for the case when the argument is greater than the order, he derived the following:

$$J_\nu(\nu \sec \beta) = \frac{1}{3} \tan \beta \cos \left[ \nu \left( \tan \beta - \frac{1}{3} \tan^3 \beta - \beta \right) \right] \left( J_{-\frac{1}{3}} + J_{\frac{1}{3}} \right) + 3^{-\frac{1}{2}} \tan \beta \sin \left[ \nu \left( \tan \beta - \frac{1}{3} \tan^3 \beta - \beta \right) \right] \left( J_{-\frac{1}{3}} - J_{\frac{1}{3}} \right) + 24\theta_2 \nu^{-1} \quad (18)$$

where  $|\theta_2| < 1$  and the argument for the Bessel functions  $J_{\pm\frac{1}{3}}$  is  $\frac{1}{3}\nu \tan^3 \beta$ . The great advantage of these formulae is that they have error bounds given. We have found that  $|\theta_1|$  and  $|\theta_2|$  do not generally have constant values for different values of the argument, but they do nevertheless stay below 1. We have plotted the values of  $\theta_1$  and  $\theta_2$  such that Watson’s expansion matches the exact value, for a range of arguments with  $\nu = 300$  (Figure 1). From these graphs, it is clear that  $|\theta_1|$  stays below  $\sim 0.0052$  and  $|\theta_2|$  stays below  $\sim 0.0016$ .

On the other hand, Debye [19] introduced what we will term as the “ $\epsilon$  expansion”. The idea is motivated by introducing a small parameter  $\epsilon$ , such that  $\nu = x(1 - \epsilon)$ , where  $\nu$  denotes the order and  $x$  is the argument of the Bessel function. This expansion is given below:

$$J_\nu(x) \sim \frac{1}{3\pi} \sum_{m=0}^{\infty} B_m(\epsilon x) \sin \left[ \frac{1}{3}(m+1)\pi \right] \cdot \frac{\Gamma(\frac{1}{3}m + \frac{1}{3})}{(\frac{1}{6}x)^{(m+1)/3}} \quad (19)$$

We extended this analysis of Debye by 5 orders to the terms  $B_m(\epsilon x)$ ,  $m = 0, 1, 2, \dots, 15$  [9]. It should be remarked that the single value of the Bessel function when the argument equals the order ( $x = \nu$ ) was also considered in this earlier study which extended the previous work of [20] by two orders. We observed that inclusion of the higher order terms leads to highly accurate values, and so the singular case, for the uniform expansions (when  $x = \nu$ ) is well under control.



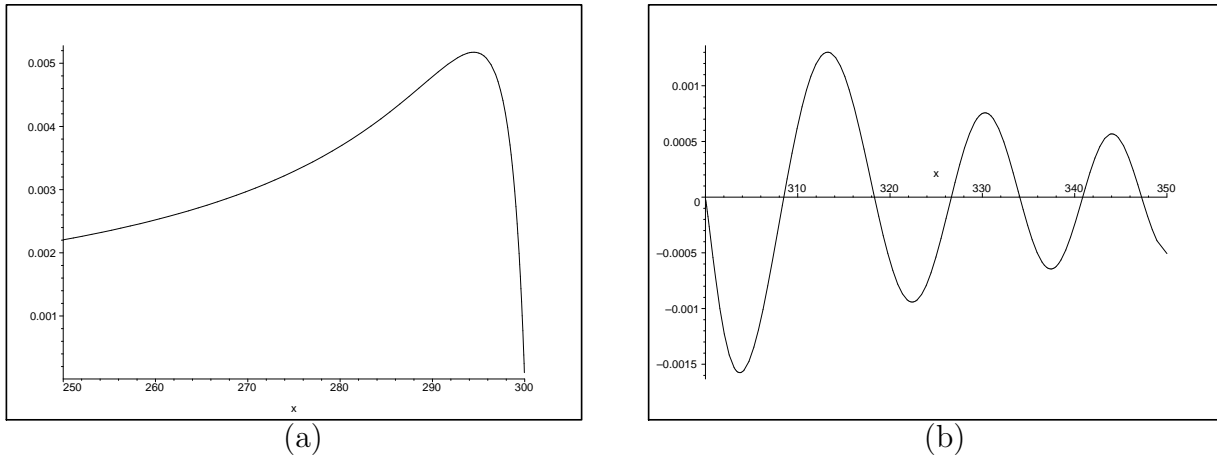


Figure 1: Plots of calculated values of (a)  $\theta_1$  and (b)  $\theta_2$  vs. the argument of the Bessel function, for order  $\nu = 300$ .

Now, to illustrate the applicability of these three methods to the transition region ( $z \sim 1$ ), we present Figures 4 and 5, which are plotted for the problematic regions relevant for GW phenomenology (when the order is as large as  $\nu = 1000000$ ). Watson's expansion and the  $\epsilon$  expansion both show remarkable ability in capturing the functions in the transition region.

We were not able to make exact comparison for such a large order, obviously due to massive computer times required. However, in Figures 4 and 5, we observe strong evidence that the proposed uniform Bessel asymptotic expansions are appropriate for GW signal analysis. Here, we note the transition region starting at values of the argument at 1,000,000 and going up to 1,000,200. In this region, the  $\epsilon$  expansion, Watson's formula and the uniform expansion closely coincide with one another. As we found earlier [9] the  $\epsilon$  expansion breaks down earlier as the argument leaves the transition region; however, all three methods coincide in a certain region indicating that we have consistent methods that work for values relevant to GW analysis. The uniform Bessel expansion is fairly easy to implement computationally and indicates good stability for rather large values of the argument. To illustrate the type of values a GW pulsar FT would require, we present Figure 6. Here, we plot the uniform Bessel expansion for values ranging from 1,000,200 to 32,500,000, which are relevant for GW phenomenology. This appears as a black band and is a continuous function which indicates oscillations tightly bunched together, and happens to be identical to a graph obtained earlier by using Meissel's second expansion [9]. It is noteworthy that the method is stable and shows consistent behaviour over an extreme range of values for the argument.

The zeroes (roots) of the Bessel function will help to identify the sky locations in terms of  $\theta$  where the signal strength is zero. Zeroes of Bessel functions arise in a variety of diffraction problems. Derivatives of Bessel functions are also important in a multitude of applications and are evaluated using the uniform expansions.

It is worth mentioning here a procedure developed by Baruth [21] which can evaluate Bessel functions for large index and argument, for example in the range of 5 million. The procedure performs evaluations in less than 10 ms, and the author believes that it can be improved even further. As an example, he has calculated  $J_{1000000}(999995) = 4.267834146855037 \times 10^{-3}$ , which is close to our value of  $4.267834146855055 \times 10^{-3}$ , an agreement of 13 decimal places.

### Number-theoretic study of the denominators of $u_i$

We note here an interesting pattern regarding the functions  $u_i$  used in the uniform expansion. Using MAPLE we undertook a study of the denominators occurring in the  $u_i$  mainly because their prime number factorizations appear to have some surprising properties.

Let  $d_i$  denote the common denominator of the terms of  $u_i$  for  $i = 0, 1, \dots$  and consider the prime number factorizations of the first eleven  $d_i$ 's :

$i$	$d_i$	
0	1	
1	$2^3 3$	
2	$2^7 3^2$	
3	$2^{10} 3^4 5$	
4	$2^{15} 3^5 5$	(20)
5	$2^{18} 3^6 5 7$	
6	$2^{22} 3^8 5^2 7$	
7	$2^{25} 3^9 5^2 7$	
8	$2^{31} 3^{10} 5^2 7$	
9	$2^{34} 3^{13} 5^3 7 11$	
10	$2^{38} 3^{14} 5^3 7^2 11$	

### Powers of 2

Let  $a_i$  denote the exponent of 2 in the prime number factorizations of  $d_i$  for  $i = 0, 1, \dots$ . Then the following formula for  $a_i$  seems to be valid

$$a_i = \log_2 \left( \frac{2^{4i}}{g_i} \right) \tag{21}$$

where  $g_i$  is Gould's sequence, see [22], defined as the highest power of 2 dividing the central binomial coefficient  $\binom{2i}{i}$ . All terms of Gould's sequence  $g_i$  are powers of two and therefore  $a_i$  will be an integer. This remarkable identification was done via N. J. A. Sloane's *On-Line Encyclopedia of Integer Sequences*, see [23].

The table below lists the first eleven values given by formula (21) which agree with the values given in the previous table (20).

$i$	0	1	2	3	4	5	6	7	8	9	10
$g_i$	$2^0$	$2^1$	$2^1$	$2^2$	$2^1$	$2^2$	$2^2$	$2^3$	$2^1$	$2^2$	$2^2$
$a_i$	0	3	7	10	15	18	22	25	31	34	38

### Powers of 3

Let  $b_i$  denote the exponent of 3 in the prime number factorizations of  $d_i$  for  $i = 0, 1, \dots$ . Then the following formula for  $b_i$  seems to be valid

$$b_i = i + \text{exponent of the highest power of 3 dividing } i! \tag{22}$$

The table below lists the first eleven values given by formula (22) which agree with the values given in (20).

$i$	0	1	2	3	4	5	6	7	8	9	10
exponent	0	0	0	1	1	1	2	2	2	4	4
$b_i$	0	1	2	4	5	6	8	9	10	13	14

These number theoretic properties could potentially be useful toward finding an analytic solution to the integro-differential equation describing the Bessel function for the uniform asymptotic expansions.

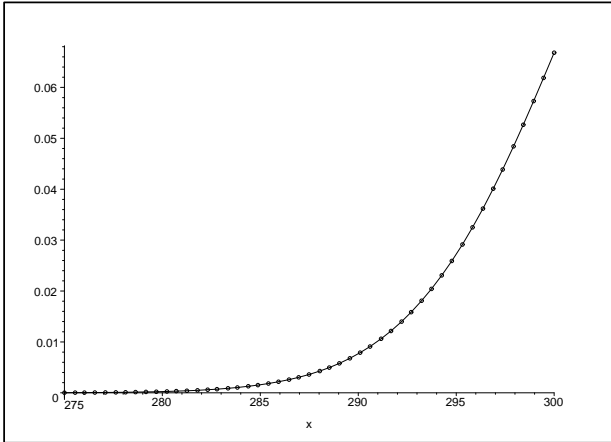


Figure 2: Uniform Bessel expansion and actual Bessel function graphed for argument  $x$  and order  $\nu = 300$  near the transition region. Solid line indicates actual Bessel function values and circles indicate values given by the expansion.

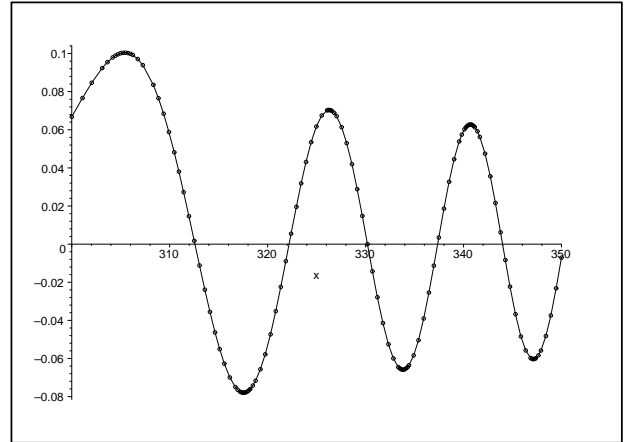


Figure 3: Uniform Bessel expansion and actual Bessel function graphed for argument  $x$  and order  $\nu = 300$  near the transition region. Solid line indicates actual Bessel function values and circles indicate values given by the expansion.

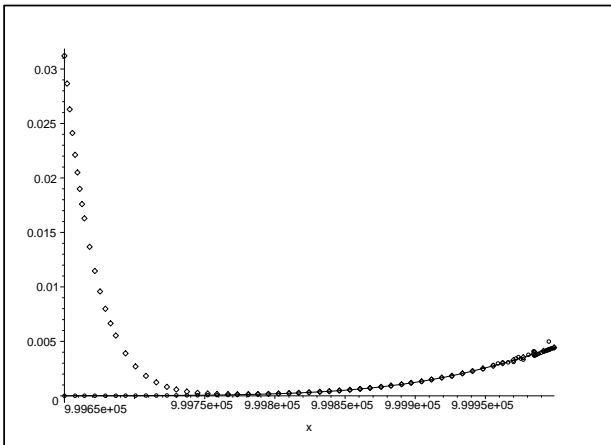


Figure 4: Comparison of uniform expansion,  $\epsilon$  expansion and Watson's formulae for argument  $x < 1,000,000$  and order  $\nu = 1,000,000$ . Solid line indicates uniform Bessel expansion values, diamonds represent  $\epsilon$  expansion and circles indicate values given by Watson's formulae.

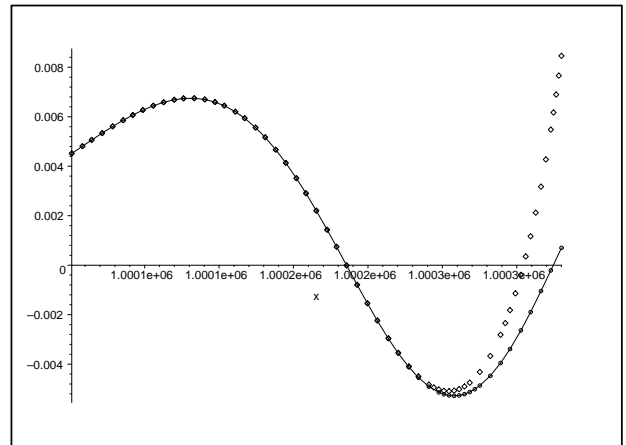


Figure 5: Comparison of uniform expansion,  $\epsilon$  expansion and Watson's formulae for argument  $x > 1,000,000$  and order  $\nu = 1,000,000$ . Solid line indicates uniform Bessel expansion values, diamonds represent  $\epsilon$  expansion and circles indicate values given by Watson's formulae.

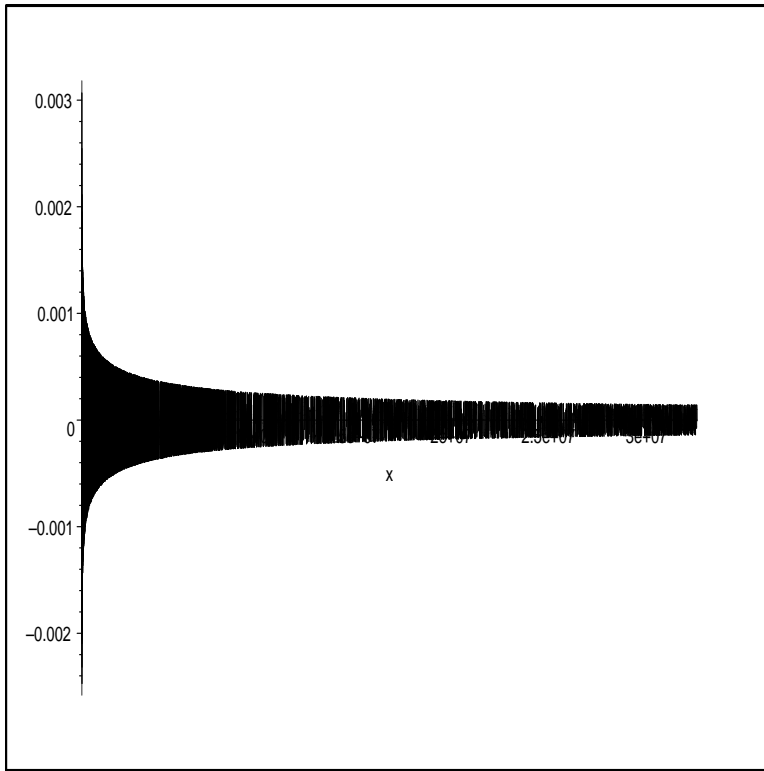


Figure 6: Plot of uniform Bessel expansion for argument  $x$  ranging from 1,000,200 to 32,500,000 for order 1,000,000.

## 5 Conclusions

In this work we examined, using symbolic computation, the accuracy and the range of validity of uniform asymptotic expansions of Bessel functions relevant for GW signal from pulsars and found them to be valid over the entire domain of the argument, including the problematic “transition region”. We compared these expansions with the fractional transition Bessel and the Debye expansions in such regions and found all three expansions to be applicable in the transition region. It was shown that there is a region where all three expansions agree, which is indicative of the accuracy of the uniform expansion in this domain.

The functions used by Bessel in 1824 in connection with planetary motion have found innumerable applications as earlier studies by Bernoulli, Lagrange, Carlini, Laplace, Poisson, Euler and many others [7] have shown. Further problems will also bring the ubiquitous Bessel functions to more diverse applications. Such applications may require accurate calculations of the functions for large order and argument, and asymptotic analysis will also be relevant for other special functions.

## 6 Acknowledgements

We are deeply grateful to SHARCNET (Shared Hierarchical Academic Research Computing Network) and NSERC for grant support. We are indebted to Dr. Nico Temme (CWI, Amsterdam) for suggesting the importance of this study and for his invaluable advice on the evaluation of the uniform expansion, and also to Dr. Dan Baruth for bringing to our attention his work on evaluation of Bessel functions of large order and argument.

## References

- [1] K. Jotania, S.R. Valluri and S.V. Dhurandhar, *Astron.Astrophys.* **306**:317,1996.
- [2] S.R. Valluri, F.A. Chishtie, et al. *Class.Quant.Grav.***19**:1327-1334,2002, Erratum-*ibid.*19:4227-4228,2002.
- [3] Valluri S. R., Chishtie F. A. and Vajda A. *Classical and Quantum Gravity*, **23**, 3323-3332 (2006).
- [4] MacPhie, R.H. and Wu, K.L., *IEEE Trans. on Antennas and Propagation*, vol.51, No.10, pp.2801-2805, 2003.
- [5] Thorne, K.S., “Multipole expansions of gravitational radiation”, *Reviews of Modern Physics*, vol.52, pp. 299-339, 1980.
- [6] Allen, B. and Ottewill, A.C. Detection of Anisotropies in the Gravitational-Wave Stochastic Background. *Phys. Rev. D* **56**:54563
- [7] Watson, G.N., *A treatise on the theory of Bessel Functions*, Cambridge University Press, 1958; *Proc. Camb. Phil. Soc.* vol. XIX, 96, 1918.
- [8] Meissel, D.F.E, “Neue Entwicklungen ueber die Bessel’schen Functionen” *Astr. Nach.* vol. CXXIX col. 281-284, 1892; *Astr. Nach.* vol. CXXX , “Weitere Entwicklungen ueber die Bessel’schen Functionen”, col. 363-368, 1892; “Einige Entwicklungen die Bessel’schen I-Functionen betreffend” vol. CXXVII, col. 359-362, 1891; “Beitrag zur theorie der allgemeinen Bessel’schen Functionen” vol. CXXVIII (1891), col.145-154.
- [9] Chishtie, F.A., Valluri S.R., Rao K.M., Sikorski, D.J., and Williams, T., IEEE Computer Society Press, Proc. 19th Annual Symposium, High Performance Computing Systems & Applications. (HPCS 2005), Guelph, Ont., Canada.
- [10] Abramowitz, M. and Stegun, I.A., *Handbook of Mathematical Functions*, National Bureau of Standards, 1964.
- [11] Prix, R. and Itoh, Y. “Global parameter-space correlations of coherent searches for continuous gravitational waves”. *Classical Quantum Gravity* **22**:S1003-S1012 (2005).
- [12] Peters P. C. and Mathews J., “Gravitational Radiation from Point Masses in a Keplerian Orbit”, *Phys. Rev.* vol. 131, pp. 435-439, 1963; Barack, L. and Cutler, C., “LISA Capture Sources: Approximate Waveforms, Signal-to-Noise Ratios, and Parameter Estimation Accuracy” *Phys.Rev. D* vol. 69, 082005, 2004.
- [13] Pierro, V., Pinto, I.M., Spallicci, A.D., Laserra, E. and Recano, F., *Mon. Not. R. Astron. Soc.* **325**:358-372 (2001).
- [14] Berry, M.V. and Mount, K.E., *Rep. Progr. Phys.* **35**, 315 (1972).
- [15] Ford, K.W. and Wheeler, J.A., *Ann. Phys.* **7**:259, 287 (1959); Romo, W.J. and Valluri, S.R., *Physica Scripta* **71**:1-10 (2005).
- [16] Regge, T. and Wheeler, J.A., *Phys. Rev.* **108**, 1063 (1957).

- [17] Poston, T. and Stewart, I. *Catastrophe theory and its applications*, Pitman Publishing, London, 1978.
- [18] Temme, N.M., Numerical algorithms for uniform Airy-type asymptotic expansions, *Numerical Algorithms* 15, 207 - 225 (1997).
- [19] Debye, P., "Naeherungsformeln fuer die Zylinderfunktionen fuer grosse Werte des Arguments und unbeschraenkt veraenderliche Werte des Index", *Math. Ann.*, vol. LXVII pp.535-558, 1909.
- [20] Airy, J.R. "Bessel and Neumann Functions of Equal Order and Argument" *Phil. Mag.* (6) vol. XXXI, 520-528, 1916.
- [21] Baruth, D., Bessel Functions of Large Orders and Arguments. World Wide Web URL [www.iging.com/transcendental/J\\_1000000.htm](http://www.iging.com/transcendental/J_1000000.htm)
- [22] J.-P. Allouche and J. Shallit, The ring of k-regular sequences, *Theoretical Computer Sci.*, 98 (1992), 163-197.
- [23] N. J. A. Sloane, The On-Line Encyclopedia of Integer Sequences. World Wide Web URL [www.research.att.com/~njas/sequences/](http://www.research.att.com/~njas/sequences/)